Covalent Modification of G-Actin by Pyridoxal 5'-Phosphate: Polymerization Properties and Interaction with DNase I and Myosin Subfragment 1

Cécile Combeau and Marie-France Carlier*
Laboratoire d'Enzymologie du CNRS, 91198 Gif-sur-Yvette Cedex, France
Received July 22, 1991; Revised Manuscript Received September 24, 1991

ABSTRACT: Pyridoxal 5'-phosphate (PLP), a lysine-specific reagent, has been used to modify G-actin. At pH 7.5, PLP reacted with 1.7–2 lysines on G-actin. Limited proteolytic digestion experiments indicated that, in agreement with previous works, essentially lysine-61 was modified in a 1:1 fashion by PLP, other lysines being much less reactive. A PLP-derivatized affinity label of ATP binding sites, AMPPLP, reacted with two additional lysines that do not appear to be located in the ATP site on G-actin. PLP–G-actin did not polymerize spontaneously up to 30 μM; however, it retained other essential native properties of G-actin. PLP–actin bound to the barbed ends of actin filaments with an equilibrium dissociation constant of 4 μM and prevented dilution-induced depolymerization like a capping protein. PLP–actin copolymerized with unmodified actin. The stability of F-actin copolymers decreased with the fraction of PLP–actin incorporated, consistent with a model within which the actin–PLP–actin interactions in the copolymer are 50-fold weaker, and PLP–actin–PLP–actin interactions are 200-fold weaker than regular actin–actin interactions. PLP–actin bound DNase I with an equilibrium association constant of 2 nM^{-1}, i.e., 10-fold lower than that of unmodified actin. PLP modification did not affect the binding of G-actin to myosin subfragment 1. However, polymerization of PLP–actin by myosin subfragment 1 was not observed in low ionic strength buffers, whereas PLP–F-actin–S_1 filaments, in which the stoichiometry PLP–actin:S_1 is 1:1, were formed with an apparent critical concentration of 4.5 μM in the presence of 0.1 M KCl.

Chemical modification of actin has been widely used to probe the regions of this protein that are in contact with actin binding proteins or that are part of the actin–actin interaction areas in the filament. Lysine residues have been shown to be involved in actin polymerization. Among the 19 lysine residues in actin, several lysines, located mainly in a region spanning residues 40–69 and possibly extending to residue 113, appeared less accessible to acetic or maleic anhydride in F-actin than in G-actin (Lu & Szilagyi, 1981; Hitchcock-De Gregori et al., 1982; Burtnick, 1984; Waring & Cooke, 1987; Sutoh, 1984). Within this region, lysine-61 has been shown to be the main residue labeled by fluorescein isothiocyanate (FITC). In addition FITC labeling impaired the polymerization of G-actin (Ng & Burtnick, 1982; Miki, 1987, 1989; Miki & Dos Remedios, 1988; Miller et al., 1988a). These data are consistent with the 3D structure of G-actin at atomic resolution (Kabsch et al., 1990) and the derived model of the actin filament (Holmes et al., 1990) showing that lysine-61 is exposed at the pointed end of the filament, where it can interact with DNase I, in agreement with independent reports (Podolski & Steck, 1988). Lys-61 appears important in maintaining the conformation of the flexible loop 37–52, which appears involved in the actin–actin interactions along the long pitch helix of the filament. Specific chemical modification of this area of actin–actin interaction may lead to a nonpolymerizable actin molecule that would keep intact its ability to interact with other proteins.

Of special interest, in this respect, is the actin–myosin interaction. It is accepted that a change in the conformation of the actomyosin complex, coupled to ATP hydrolysis, provides the molecular basis for muscle contraction. The binding of the myosin head to actin filaments can be understood within the general frame of binding of a ligand to interacting sites; therefore, it is possible that (1) actin–actin interactions can be modified by S_1 binding and (2) changes in actin–actin interaction may also occur during muscle contraction. To understand in detail which kind of actin–actin contacts may be involved in actin–myosin motility, it is important to make tools such as actin modified specifically on one such actin–actin interaction area.

In this work, we have used pyridoxal 5'-phosphate (PLP)[1] to modify lysine-61 on G-actin. The adduct retains the native properties of G-actin but is unable to polymerize up to 30 μM. PLP–G-actin can, however, copolymerize with unmodified G-actin. The kinetics and thermodynamics of copolymers of actin and PLP–actin have been studied quantitatively. PLP–G-actin binds to DNase I with a 10-fold reduced affinity; it forms with myosin subfragment 1 a ternary G_2S and a binary GS complex with the same affinity as unmodified G-actin. Myosin subfragment 1 (S_1) can induce polymerization of PLP–actin only in high ionic strength buffers, with a critical concentration high enough to enable an easier approach of the mechanism of S_1-induced polymerization of G-actin.

Materials and Methods

Chemicals. ATP, dithiothreitol, and DNase I (grade II) came from Boehringer Mannheim; pyreneiodoacetamide was from Molecular Probes. α-Chymotrypsin was purchased from Worthington. Thrombin (from bovine plasma), HEPES, $NaBH_4$, adenosine 5'-phosphomorpholidate and PLP were from Sigma. Stock solutions of PLP (30–50 mM) were brought to pH 7.0 with NaOH and kept at −20 °C in the dark. The concentration of PLP was determined using an extinction coefficient of 6600 M^{-1} cm^{-1} at 388 nm in 0.1 N NaOH. [2,8-^{3}H]ATP and [^{3}H]$NaBH_4$ were from Amersham. AMP-PLP was synthesized from PLP and adenosine 5'-

[1] Abbreviations: HEPES, 4-(2-hydroxyethyl)-1-piperazineethanesulfonic acid; PLP, pyridoxal 5'-phosphate; AMP–PLP, pyridoxal(5')diphospho(5')adenosine; $NaBH_4$, sodium borohydride; EDTA, (ethylenedinitrilo)tetraacetic acid; PMSF, phenylmethanesulfonyl fluoride; SDS–PAGE, sodium dodecyl sulfate–polyacrylamide gel electrophoresis.

0006-2960/92/0431-300$03.00/0

phosphomorpholidate as described (Tamura et al., 1986) with the following modification. DEAE-cellulose chromatography of the products was carried out in 20 mM triethylammonium carbonate buffer, pH 7.5, with a 20–50 mM triethylammonium carbonate gradient. The fractions containing AMP–PLP were pooled. The product was then concentrated, and TEA was evaporated using a rotary evaporator (Büchi). This procedure yielded a salt-free 30 mM solution of AMP–PLP. The product was stable at −20 °C for at least 2 months.

Protein Purification. Actin was purified from rabbit muscle acetone powder (Spudich & Watt, 1971; Eisenberg & Kielley, 1974) and isolated as CaATP–G-actin through Sephadex G-200 chromatography (McLean Fletcher & Pollard, 1980) in buffer G (5 mM Tris-HCl, pH 7.8, containing 0.2 mM dithiothreitol, 0.2 mM ATP, 0.1 mM $CaCl_2$, and 0.01% sodium azide). G-actin (40–50 μM) was stored on ice and used within two weeks. [^{3}H]ADP–G-actin was prepared by polymerizing [^{3}H]ATP–G-actin and resuspending the pellets of F-actin–[^{3}H]ADP in buffer G containing no ATP, followed by a 10-min centrifugation at 400000*g* (TL 100, Beckman) to eliminate any residual F-actin. Pyrenyl-labeled (Kouyama & Mihashi, 1981) actin was used as a fluorescent probe of the polymerization process.

Myosin was purified from rabbit muscle as described (Offer et al., 1973) up to the ammonium sulfate fractionation, followed by extensive dialysis against 0.15 M phosphate buffer, pH 7.0, containing 10 mM EDTA. Myosin was then supplemented with 50% glycerol and stored at −20 °C at 8–12 mg/mL.

Myosin subfragment 1 (S_1) was prepared by chymotryptic digestion of myosin (Weeds & Pope, 1977) and further resolved into S_1A_1 and S_1A_2 isomers by DEAE-cellulose chromatography (Weeds & Taylor, 1975). Solutions of S_1 were kept on ice and used within two weeks.

DNase I was dissolved in 50 mM Tris-HCl, pH 7.5, containing 0.01 mM PMSF and 0.1 mM $CaCl_2$ and used the same day.

α-Chymotrypsin was dissolved in distilled water and thrombin in 0.15 M NaCl.

Protein concentrations were determined spectrophotometrically using the extinction coefficients $\epsilon_{290}^{0.1\%} = 0.617$ cm^{-1} for actin (Gordon et al., 1976), $\epsilon_{280}^{0.1\%} = 0.74$ cm^{-1} for S_1A_1 (Margossian & Lowey, 1982), $\epsilon_{280}^{0.1\%} = 0.75$ cm^{-1} for S_1A_2 (Margossian & Lowey, 1982), and $\epsilon_{280}^{0.1\%} = 1.23$ cm^{-1} for DNase I (Hitchcock et al., 1976) and the molecular masses 42 kDa (actin), 112 kDa (S_1A_1), 105 kDa (S_1A_2), and 31 kDa (DNase I).

Nucleotide Exchange on G-Actin. Exchange of AMP–PLP or ATP for [^{3}H]ADP bound to G-actin was measured using a Dowex-1 assay (AG1-X8, 200–400 mesh, Bio-Rad). Samples of 0.1 mL of [^{3}H]ADP–G-actin (15 μM) were incubated with desired amounts of ATP, AMP–PLP, or PLP for 3 min at 0 °C. This period of time was found sufficient for the complete dissociation of ADP, which is known to be rapid (Nowak & Goody, 1988; Frieden & Patane, 1988). A total of 0.1 mL of a 50% Dowex-1 suspension was then added to trap all free nucleotides or PLP. The Dowex resin was rapidly sedimented at 10000*g* for 1 min, and the amount of [^{3}H]-ADP–G-actin present in the supernatant was determined by radioactivity measurement.

Modification of G-Actin by PLP or AMP–PLP. G-Actin (20–30 μM) was equilibrated in buffer H, i.e., buffer G in which Tris, which reacts slowly with PLP, was replaced by HEPES. Routinely, 3 mM PLP was reacted for 1 h with G-actin at 20 °C under dim light. The Schiff base was reduced by addition of 10 mM $NaBH_4$. Unbound reagent and excess $NaBH_4$ were removed by overnight dialysis against buffer G, followed by Sephadex G-25 chromatography (PD-10, Pharmacia).

The amount of PLP or AMP–PLP covalently incorporated into G-actin following incubation with different concentrations of reagent and reduction of the Schiff base was determined by two independent methods as follows. The reduced PLP–G-actin was extensively dialyzed against buffer G and chromatographed through Sephadex G-25 (PD-10, Pharmacia) equilibrated in buffer G without nucleotide, to remove ATP, residual $NaBH_4$, and unbound reduced PLP. The amount of PLP covalently bound to G-actin was determined spectrophotometrically using an extinction coefficient for the reduced Schiff base of 8800 M^{-1} cm^{-1} at 323 nm (Dempsey & Snell, 1963). In the second method, 100-μL samples of G-actin (15–20 μM) were incubated for 1 h in the presence of PLP or AMP–PLP in a range of concentrations from 0 to 5 mM. Following reduction by 10 mM [^{3}H]$NaBH_4$ (0.5 Ci/mol), the protein was denatured by the addition of 4 mL of ice-cold 10% trichloroacetic acid, to which BSA (0.1 mg/mL) was added as a carrier. The solution containing the precipitated protein was filtered through GFC filters (Whatman) followed by extensive washings with 10% TCA. The filters were put in scintillation vials and incubated for 30 min with 0.5 mL of 0.5 M NaOH, and radioactivity was counted in 10 mL of Aquasol using a Packard 2000 CA liquid scintillation spectrometer. The molar amount of [^{3}H]PLP incorporated per mole of actin was derived from the measurement of ^{3}H radioactivity covalently incorporated in the protein. The calculation was carried out taking into account the fact that ^{3}H-labeled $NaBH_4$ consists of a mixed population of heterogeneously labeled molecules containing 1–4 ^{3}H atoms/molecule. A typical batch of [^{3}H]$NaBH_4$ contained 28% monotritiated, 30% ditritiated, 30.2% tritritiated, and 11.8% tetratritiated [^{3}H]$NaBH_4$; 1 mol of $NaBH_4$ therefore contains 2.26/4 = 0.565 mol of reactive ^{3}H.

Limited Proteolytic Digestion of [^{3}H]PLP–G-Actin (Mornet & Ue, 1984). [^{3}H]PLP–G-actin (1 mg/mL) obtained by reduction of the Schiff base with 10 mM [^{3}H]$NaBH_4$ was incubated at 20 °C in buffer G in the presence of 0.1 mg/mL α-chymotrypsin. Aliquots of 200 μL were removed from the solution every 2 min and supplemented with 5 mM PMSF to stop the proteolytic digestion. Alternatively, [^{3}H]PLP–G-actin (1 mg/mL) was treated by thrombin (20 units/mL) at 25 °C in buffer G containing 0.5 mM EDTA. Aliquots of 200 μL were withdrawn every 30 min and immediately denatured by boiling for 5 min in the presence of 2% SDS. The proteolysis products were separated by SDS–PAGE on slab gels (Laemmli, 1970) using a 10–18% acrylamide gradient and 50 mM Tris/100 mM boric acid, pH 8.0, as running buffer (Mornet & Ue, 1984). Electrophoresis was carried out overnight under a constant voltage of 50 V.

Gel Autoradiography. Coomassie blue stained gels of the electrophoresed proteolytic fragments of [^{3}H]PLP–actin were treated with Entensify (NEN). The slabs were laid onto Bio-Rad backing paper and dried under vacuum. The dried gels were then autoradiographed using a Kodak X-O-MAT AR film and 7 days of exposure at −80 °C. Both the Coomassie blue stained gels and the corresponding autoradiograms were digitalized using a camera (Pasecon, LHESA Electronics) attached to an image-analysis instrument (CYTIX, Digital Design). A linear scale of the gray levels was derived. Several amounts of material present in a given sample were deposited on the gels. Each polypeptide band was identified

both on the Coomassie blue pattern and on the autoradiogram. For each polypeptide band, linear dependences of the integrated intensities of the Coomassie blue stain and of the corresponding autoradiogram spot, versus the amount of protein loaded, were obtained; the linearity testified that all measurements of protein mass (from Coomassie blue stain) and of radioactivity were made in a subsaturating range in the gray scale. The ratio of the slopes of these two straight lines represented the amount of covalently incorporated [^{3}H]PLP per mass unit of the considered polypeptide. It was implicity assumed, in this analysis, that Coomassie blue stained each fragment of actin identically.

Polymerization Measurements. Actin polymerization was monitored by the increase in fluorescence of the covalently attached pyrenyl probe, using a Spex Fluorolog 2 spectrofluorometer, equipped with a DM1B datamate. The rate of elongation of F-actin filaments in the presence of G-actin subunits was monitored by pyrenyl fluorescence as previously described (Carlier et al., 1984). A small aliquot of a pyrenyl-labeled F-actin solution (25 μM actin) was added, as seeds, to a solution of identically labeled G-actin, at a given concentration, in polymerization buffer. The initial rate of pyrenyl fluorescence change was measured.

Polymerization of actin induced by S_1A_1 was followed by light scattering. Prior to the measurements, all the solutions were passed through a 0.22-μm Millipore filter and the protein solutions were clarified by a 10-min centrifugation at 4 °C and 350000g in a Beckman TL100 ultracentrifuge. Light scattering intensity was measured at 90° with a 600-nm-wavelength unpolarized light.

Alternatively, the amount of polymer formed was determined in a sedimentation assay. F-Actin sedimented in 30 min at 4 °C and 400000g whereas F-actin–S_1A_1 sedimented in 10 min under the same conditions. The amount of proteins in the supernatant was determined by a Bradford assay. The S_1:actin ratio in the pellets was estimated by SDS–PAGE.

Binding of DNase I to G-Actin. The binding of DNase I to PLP-modified and unmodified G-actin was derived from the extent of inhibition of DNase I activity by G-actin (Blikstad et al., 1978). The hydrolysis of DNA was followed by the hyperchromicity at 260 nm (Kunitz, 1950), using a Cary 219 spectrophotometer, under conditions where the increase in absorbance was linear with time and proportional to the amount of DNase I in the assay. The percent inhibition observed in the presence of a given concentration of G-actin was linearly related to the proportion of actin-bound DNase I.

Results

Modification of G-Actin by PLP. When PLP (0.2–0.5 mM) was reacted with CaATP–G-actin in buffer H, a visible difference spectrum slowly developed in the 300–500-nm region, with a maximum hyperchromicity at 432 nm, a minimum at 380 nm, and isosbestic point at 405 nm, indicating the formation of a Schiff base between PLP and actin (Matsuo, 1957). Advantage was taken of the absorbance change at 432 nm to follow the kinetics of modification of G-actin by PLP. PLP reacted with G-actin within a pseudo-first-order process. The apparent first-order rate constant exhibited a hyperbolic dependence on PLP concentration, consistent with a mechanism in which a rapid equilibrium between G-actin and PLP (K_D = 80 μM) precedes the slow isomerization of the complex (k_i = 0.003 s^{-1}) into a compound in which the Schiff base absorbs (data not shown). The extent of absorbance change after completion of the reaction showed a saturation behavior with the concentration of PLP. Covalent binding of PLP to

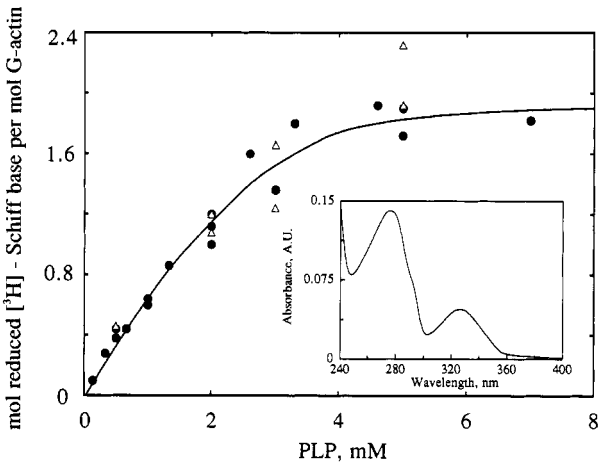

FIGURE 1: Amount of PLP covalently incorporated in G-actin. G-Actin (15–20 μM) in buffer H was reacted with PLP at the indicated concentrations for 1 h at 20 °C. The amount of PLP covalently bound to actin was determined by a TCA assay following reduction of the Schiff base by [^{3}H]$NaBH_4$ (see Materials and Methods). The experiment was done with CaATP–G-actin (●) and CaADP–G-actin (△). Inset: Absorption spectrum of PLP–actin (13.8 μM) following reaction with 3 mM PLP, reduction by $NaBH_4$, and Sephadex G25 chromatography (see Materials and Methods).

G-actin was achieved by reducing the Schiff base by $NaBH_4$. The amount of PLP covalently incorporated in G-actin was derived (see Materials and Methods) from the absorbance of the pyridoxamine derivative at 323 nm, and from the covalent incorporation of ^{3}H following reduction of the Schiff base with [^{3}H]$NaBH_4$. The results of these two determinations, shown in Figure 1, were consistent with each other. Reaction of G-actin with 3 mM PLP led to the covalent incorporation of 1.89 PLP/actin from the UV–visible spectrum and 1.7 PLP/per actin from ^{3}H measurements. The same result was obtained with ADP–G-actin, which however, reacted faster than ATP–G-actin with PLP.

Localization of the PLP-Modified Lysines on Actin by Proteolytic Digestion. To identify the actin sequences that carry the covalently bound PLP, the [^{3}H]PLP-modified protein was subjected to limited proteolytic digestion by either thrombin or α-chymotrypsin (Mornet & Ue, 1984). The thrombin hydrolysates were analyzed by gel electrophoresis (Figure 2A) and autoradiography (Figure 2B). Thrombin splits unmodified as well as PLP-modified actin into two major fragments of 10 and 27 kDa, which correspond to sequences 40–113 and 114–375, respectively (Muszbek et al., 1975). Analysis of the amount of ^{3}H in the 10- and 27-kDa fragments (Figure 2C) showed that the amount of bound PLP per protein mass unit was twice larger in the 10-kDa fragment spanning residues 40–113 (which contains five lysines in 73 amino acids) than in the 27-kDa fragment 114–374 (which contains 13 lysines in 260 amino acids). Therefore, at least one of the five lysines, Lys-50, -61, -68, -84, and -113 is more labeled than others. Additional experiments of limited proteolysis of PLP-modified and unmodified actin by α-chymotrypsin yielded an intermediate 35-kDa species that is further degraded into a 33-kDa fragment, both known to contain the C-terminus of actin (Mornet & Ue, 1984). It has further been shown that the N-termini of the 35- and 33-kDa fragments are Val-45 and Lys-68, respectively (Konno, 1987, 1988). The results of proteolysis of PLP–actin by α-chymotrypsin are displayed in Figure 3. Image analysis of the data (Figure 3C) shows that the amount of ^{3}H incorporated per mass unit of protein is 2.5–3-fold higher in the 35-kDa fragment than in the 33-kDa fragment. This piece of data indicates that lysine-50 and

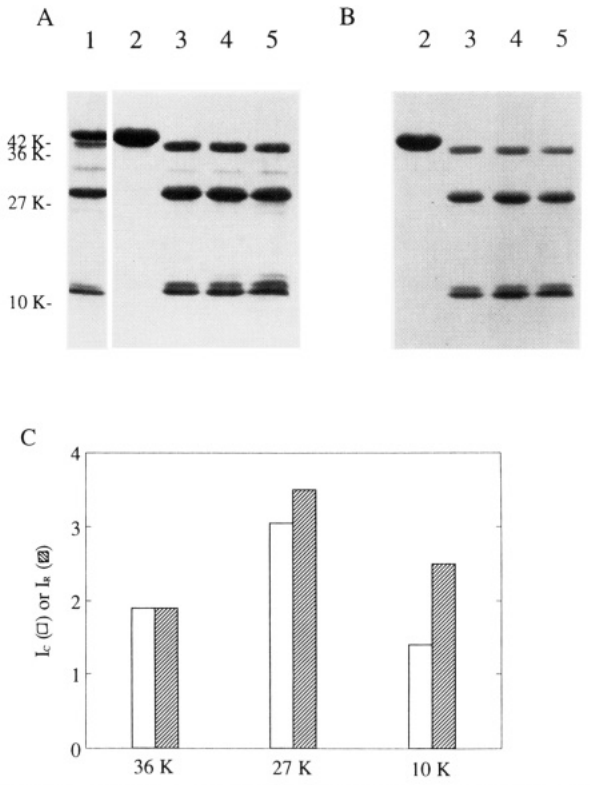

FIGURE 2: Digestion pattern of [^{3}H]PLP–G-actin by thrombin. [^{3}H]PLP–G-actin (1 mg/mL) was digested by thrombin (20 units/mL) at 25 °C in buffer G supplemented with 0.5 mM EDTA. At the times indicated, aliquots were withdrawn from the reaction mixture, denatured, and processed for gel electrophoresis. A total of 30 μg of each sample was loaded on the gel. The lanes represent (1) control sample in which unmodified G-actin was digested by thrombin for 60 min or (2–5) samples in which [^{3}H]PLP–G-actin was digested by thrombin for 0, 30, 60, and 120 min, respectively. Panel A: Coomassie blue staining pattern. Panel B: Autoradiogram of the gel shown in panel A. Panel C: Analysis of the data. For each of the three polypeptides of apparent molecular mass 36 kDa, 27 kDa, and 10 kDa, the intensities of the Coomassie blue, I_C, and of the corresponding spot on the autoradiogram, I_R, were integrated. It was found that, for each polypeptide, the ratio I_R to I_C, was the same within 10% at the three digestion times. The histogram therefore shows the average integrated intensities I_C (open bars) and I_R (hatched bars) for each polypeptide.

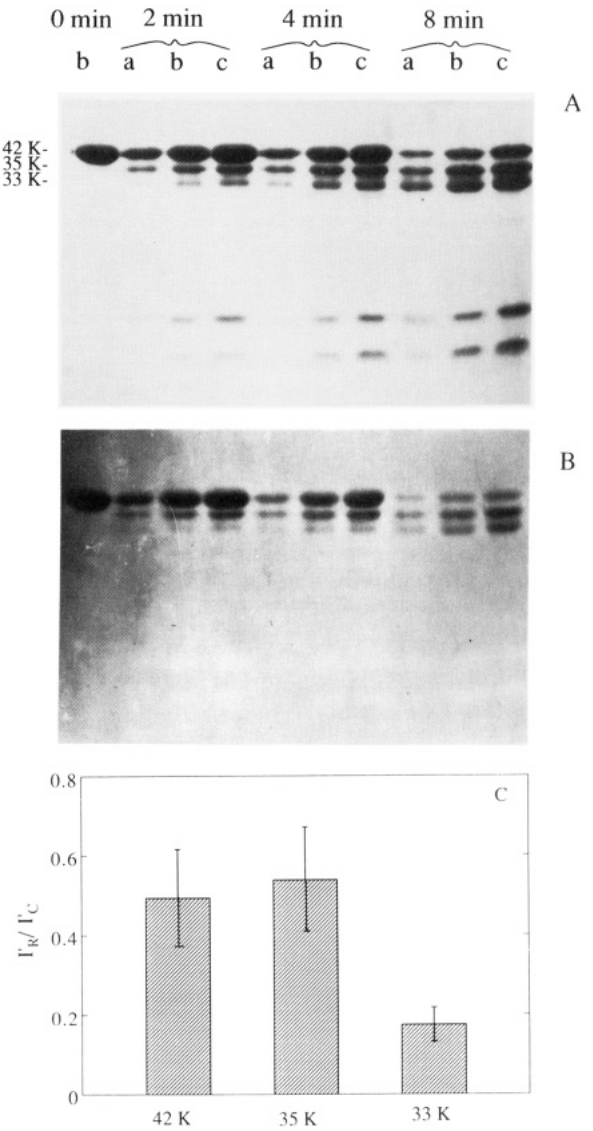

FIGURE 3: Limited digestion of [^{3}H]PLP–G-actin by α-chymotrypsin. [^{3}H]PLP–G-actin (1 mg/mL) was digested by α-chymotrypsin (0.1 mg/mL). At the times indicated, aliquots were withdrawn from the reaction mixture, denatured, and processed for gel electrophoresis. For each time point, 15 μg (lane a), 30 μg (lane b), or 60 μg (lane c) of protein was deposited on the gel. Panel A: Coomassie blue staining pattern. Panel B: Autoradiogram of the gel shown in panel A. Panel C: Analysis of the data. For each of the three polypeptides of mass 42 kDa, 35 kDa, and 33 kDa, and at each digestion time, linear dependences of the integrated intensities I_C and I_R on the amount of protein loaded were established. The derived slopes represent the reduced intensities I'_C and I'_R per protein mass unit. Values of I'_C and I'_R were thus obtained at each digestion time, for each polypeptide. The histograms shows the ratio I'_R to I'_C for the three polypeptides. The error bar accounts for the deviation from the average value over the three digestion times. The data demonstrate that the specific radioactivity of the 33-kDa species is 2.5-fold lower than that of the 42-kDa and 35-kDa species.

lysine-61, which are the only lysines of actin between residues 45 and 67, must carry at least 60% of the covalently incorporated PLP. Other experiments described later in this paper show that PLP modification weakens the affinity of DNase I for G-actin. Since Lys-61, but not Lys-50, is part of the DNase I binding site on G-actin, we propose that lysine-61 is the major target of PLP modification. Since on the average 1.7–2.0 lysines are modified by PLP, the fact that 60% of bound PLP is found on lysine-61 indicates that all G-actin molecules have been modified on lysine-61 with a 1:1 stoichiometry. The limited proteolysis experiments using both thrombin and α-chymotrypsin suggest that the remaining 40% of incorporated PLP is scattered on many lysines of G-actin with a stoichiometry lower than 0.1 per lysine on average. FITC also has been reported to modify up to two lysines on G-actin; therefore, the conclusions that we reach here concerning PLP modification most likely also apply to FITC modification.

Absence of a Reactive Lysine Residue in the Region of the γ-Phosphate of ATP Bound to G-Actin. AMP–PLP has recently been demonstrated to be a suitable affinity label of the ATP binding sites of hexokinase and phosphoglycerate kinase (Tamura et al., 1986). The glycine-rich consensus sequence of the phosphate binding site of several ATP and GTP binding proteins also contains a lysine residue (Fry et al., 1986). In order to probe the presence of a reactive lysine in the binding region of the γ-phosphate of ATP on actin, AMP–PLP was synthesized and tested for its ability to bind to the ATP site of G-actin and to react with a lysine residue in the site. The displacement of [^{3}H]ADP bound to G-actin by ATP, AMP–PLP, and PLP was investigated using the Dowex-1 assay described under Materials and Methods. Figure 4 shows that PLP does not displace bound ADP from actin, while AMP–PLP does with a low affinity. A total of

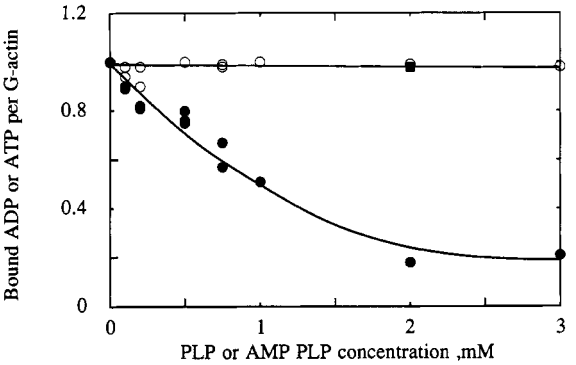

FIGURE 4: Comparison of the reactions of PLP and AMP–PLP with G-actin. Exchange of PLP and AMP–PLP for bound [^{3}H]ADP or ATP on G-actin. [^{3}H]ADP–G-actin at a concentration of 15–20 μM was incubated with PLP (○) or AMPPLP (●) at the concentrations indicated. The amount of [^{3}H]ADP–G-actin remaining in solution was measured using the Dowex-1 assay described under Materials and Methods. The solid square represents exchange of AMPPLP (2 mM) for bound [^{3}H]ATP. No exchange occurred following 1 h of incubation, while unlabeled ATP totally displaced bound [^{3}H]ATP during the same period of time.

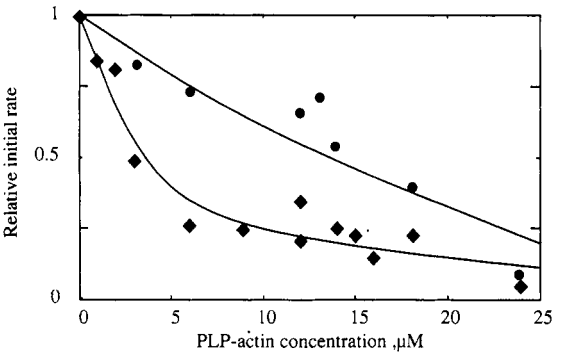

FIGURE 5: Interaction of PLP–G-actin with the barbed ends of actin filaments. A solution of F-actin (20 μM, 20% pyrenyl labeled) in buffer F (5 mM Hepes, pH 7.9, containing 0.2 mM ATP, 0.1 mM $CaCl_2$, 0.1 M KCl, and 0.2 mM DTT) was used as seeds. The initial rate of dilution-induced depolymerization was measured following a 20-fold dilution of the seeds in buffer F containing PLP–G-actin at the indicated concentrations (◆). The initial rate of filament elongation was measured following a 20-fold dilution of the seeds in buffer F containing 5 μM G-actin (20% pyrenyl labeled) and PLP–G-actin at the indicated concentrations (●). The initial rates of depolymerization or elongation measured in the absence of PLP–actin were normalized to 1.

50% of the ADP bound to 15 μM G-actin was displaced by 1 mM AMP–PLP. Since 7.5 μM ADP was then free in solution, these data indicate that AMP–PLP has a 130-fold $(1000 - 7.5)/7.5 = 130$ lower affinity than ADP for G-actin. In a separate experiment, the time courses of exchange of either ATP (2 mM) or AMP–PLP (2 mM) for actin-bound [^{3}H]ATP were compared using the same Dowex-1 assay. While unlabeled ATP exchanged for bound labeled ATP with a half-time of 10 min at room temperature, 2 mM AMP–PLP did not exchange at all for bound ATP within 1 h.

AMP–PLP, in a range of concentrations from 0 to 5 mM, was reacted with ATP–G-actin or ADP–G-actin. Following reduction by ^{3}H-labeled $NaBH_4$, the stoichiometry of AMP–PLP covalently incorporated per actin was determined by the TCA assay. A maximum of four lysines was modified by AMP–PLP both on ATP–G-actin and on ADP–G-actin (data not shown). Since AMP–PLP does not compete with ATP, these results show that none of these four lysines are located in the ATP binding site. Therefore, under conditions where AMP–PLP is bound to the nucleotide site in competition with ADP, it does not react with a lysine. The ATP site of actin therefore appears different from a large class of nucleotide binding proteins (Fry et al., 1986), while its similarity to the heat-shock cognate protein HSC 70 and to hexokinase has recently been pointed out (Holmes & Kabsch, 1991). The absence of a reactive lysine in the region of the γ-phosphate of ATP is in agreement with the 3D structure of G-actin[2] (Kabsch et al., 1990). Lys-18, which is involved in an α–β bidentate bonding with the phosphates of ATP, cannot react with the PLP moiety of AMP–PLP that actually occupies the place of the γ-phosphate of ATP. The modification of additional lysines by AMP–PLP may be due to a conformation of G-actin with AMP–PLP bound that is different from the conformation with ATP or ADP bound.

Polymerization Properties of PLP–G-actin. The ability of PLP–actin to polymerize was investigated using the pyrenyl fluorescence assay. It was first checked that pyrenyl-labeled G-actin (1 pyrenyl/actin) reacted with PLP at the same rate and to the same extent as unmodified actin, which testifies that modification of Cys-374 (at the barbed end of the G-actin molecule) does not affect the reactivity of lysine-61 (at the pointed end of the molecule). Upon addition of 0.1 M KCl, PLP–G-actin proved unable to spontaneously polymerize into filaments, up to a concentration of 30 μM, even under sonication which accelerates the polymerization process (Carlier et al., 1985). It was further checked, using the sedimentation assay, that no F-actin was formed, consistent with the absence of pyrenyl fluorescence change. PLP–G-actin also was unable to elongate onto F-actin seeds. Therefore, the inability to spontaneously polymerize was not simply due to a hampered nucleation.

Polymerizability is a major criterion for the native state of G-actin. Since PLP–G-actin does not self-assemble by itself, it was necessary to check that it is not denatured and that PLP modification has only greatly weakened the strength of actin–actin interactions without affecting other essential native properties of G-actin. It was therefore checked that PLP–actin was homogeneous in the analytical ultracentrifuge and had a sedimentation coefficient $s_{20,w}$ of 3.77 S, similar to that of unmodified G-actin and FITC–actin (Miller et al., 1988b). Therefore, PLP–actin is not aggregated.

Finally, PLP–G-actin binds ATP as tightly as unmodified G-actin: the 1:1 complex of PLP–actin with ATP can be isolated free of unbound nucleotide by Dowex-1 treatment or chromatography through Sephadex-G25 in G buffer containing no ATP. In addition, it was checked that the rate of ATP exchange for bound [^{3}H]ATP on PLP–G-actin was the same as on unmodified G-actin.

Although unable to self-assemble into filaments, PLP–actin appears able to interact with actin filaments. Figure 5 shows that PLP–G-actin inhibits the dilution-induced depolymerization of regular actin filaments with a hyperbolic concentration dependence. The data are consistent with the view that PLP–actin binds to the barbed ends of actin filaments with an equilibrium dissociation constant of 4 μM and acts like a capping protein in preventing the depolymerization of actin filaments. The observation that PLP–actin acts as a barbed end-capping protein is somewhat puzzling. Indeed, since PLP causes an alteration of the pointed end of the actin molecule, one would expect PLP–actin to be a pointed end-capping protein and to be unable to bind to the barbed end. Actually, the equilibrium dissociation constant of 4 μM found for binding of PLP actin to the barbed end is 1 order of magnitude higher

[2] While this work was in progress, the X-ray three-dimensional structure of G-actin at atomic resolution appeared, showing that no lysine was located in the site of the γ-phosphate of ATP.

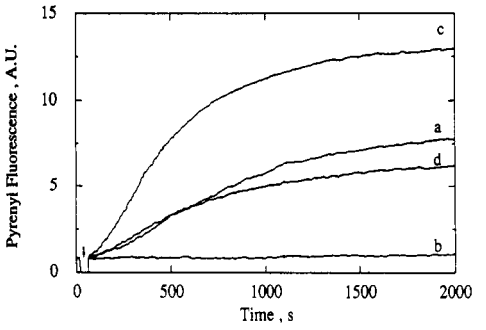

FIGURE 6: Copolymerization of PLP–actin and unmodified actin. A stock solution of G-actin containing 15% pyrenyl-actin was split in two parts, one of which was modified by PLP. Polymerization was started by addition of 0.1 M KCl and 1 mM $MgCl_2$ at time indicated by the arrow. Polymerization was monitored by the increase in pyrenyl fluorescence. The following samples were assayed: 10 μM regular G-actin (a); 10 μM PLP–G-actin (b), 10 μM G-actin + 10 μM PLP–G-actin (c); 10 μM G-actin + 10 μM PLP–G-actin (in which only PLP–actin was pyrenyl labeled) (d).

than the critical concentration for polymerization of unmodified actin. This 1 order of magnitude reduced affinity compares well with the 10-fold reduced affinity of PLP–actin for DNase I (see further below in this paper). Because the contribution of the pointed end in the overall rate of dilution-induced depolymerization off both ends is small (Carlier et al., 1986), it is not possible to detect the possible capping action of PLP–actin at the pointed end in the present experiments.

The effect of PLP–actin on the elongation of actin filaments in the presence of unmodified G-actin was also investigated. The initial rate of filament elongation was measured, as described under Materials and Methods, in the presence of 5 μM G-actin and increasing amounts of PLP–actin. Both PLP–actin and unmodified actin contained the same percent amount of pyrenyl label. Figure 5 shows that PLP–actin inhibits elongation of actin filaments; however, the concentration of PLP–actin necessary to obtain a 50% decrease in the rate of filament growth was 5-fold larger than the concentration causing half-inhibition of the rate of depolymerization upon dilution. In addition, when filament elongation was measured in the presence of varying proportions of unmodified and modified actins, the total actin concentration being held constant, the observed inhibition of growth was not consistent with a simple blockage of the barbed ends with a single equilibrium dissociation constant (data not shown). These data suggested that PLP–actin, although unable to undergo spontaneous polymerization by itself, can nevertheless copolymerize with unmodified actin. This possibility was tested in the experiment displayed in Figure 6, in which 10 μM PLP–actin (15% pyrenyl labeled) was polymerized with 10 μM unmodified G-actin (either unlabeled, curve d, or 15% pyrenyl labeled, curve c). The data show evidence for copolymerization of PLP–actin with unmodified actin, with a concomitant increase in pyrenyl fluorescence. The amount of copolymer formed can be derived both from the pyrenyl fluorescence change and from measurements of protein present in the supernatant of sedimented F-actin. Comparison of these data showed that the change in the fluorescence of pyrenyl attached to PLP–actin upon incorporation of PLP–actin into filaments was 85% of the corresponding change in fluorescence of pyrenyl attached to unmodified actin.

Since PLP–actin does not self-assemble in a range of concentration in which it can copolymerize with unmodified actin, we can expect that the stability of copolymers of unmodified regular (R) subunits and PLP-modified (P) subunits decreases upon increasing the proportion of P subunits in the filament.

Table I: Copolymerization of PLP–Actin and Unmodified Actin[a]

unmodified actin (μM)	PLP–actin (μM)	$C_{c\,app}$	proportion of PLP–actin in copolymer (γ)
3	1.5	0.87	0.17
	3	1.66	0.31
	5	3	0.40
	7.5	4.5	0.50
	10	6.06	0.56
	14	8.24	0.65
8	2	1	0.11
	4	2	0.2
	8	3.3	0.37
	10	4.5	0.41
	14.5	6.5	0.50
10	2.5	1	0.13
	5	2	0.23
	7.5	2.7	0.32
	10	3	0.41
	15	4	0.52
	22	5.3	0.62

[a] Unmodified actin at the indicated concentrations (column 1) was polymerized with PLP–actin at a series of concentrations (column 2). Both unmodified actin and PLP–actin were identically pyrenyl labeled. Polymerization was monitored by pyrenyl fluorescence. When the plateau was reached, samples were sedimented at 350000g for 20 min. Apparent critical concentrations $C_{c\,app}$ were derived from protein measurement in the supernatants.

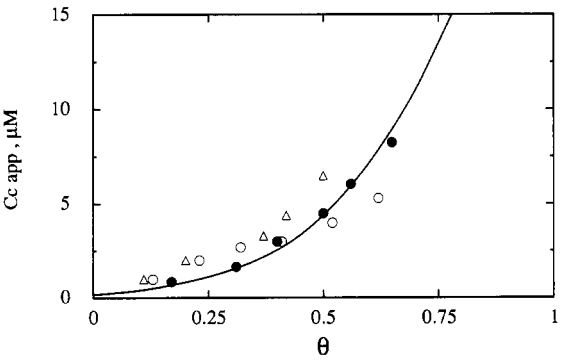

FIGURE 7: Stability of copolymers of PLP–actin and unmodified actin. Unmodified actin at a concentration of 3 μM (●), 8 μM (△), or 10 μM (○) was polymerized by addition of 0.1 M KCl in the presence of increasing amounts of PLP–actin. Apparent critical concentrations are plotted versus the fraction of PLP–actin in the copolymer, θ. Data come from Table I. The solid line represents the theoretical curve calculated according to eq 7, using $\alpha_{RP} = 0.02$ and $\alpha_{PP} = 0.005$.

This point was quantitatively documented by measuring the amount of F-actin polymerized upon addition of increasing amounts of PLP–actin to a constant amount of unmodified actin. The data, summarized in Table I and analyzed in Figure 7, show that the apparent critical concentration for the formation of F-actin copolymers increases cooperatively with the proportion of PLP–F-actin incorporated, consistent with the following model. Let ΔG_{RR}, ΔG_{RP}, and ΔG_{PP} be the free energy changes associated to the interaction between two unmodified (R) actin subunits, between an unmodified and a PLP–actin (P) subunit and between two PLP–actin subunits, respectively, and K_{RR}, K_{RP}, and K_{PP} the corresponding equilibrium association constants. The following equations describe the system (Hill, 1987), where N is Avogadro's number and k is the Boltzmann constant.

$$\Delta G_{RR} = -NkT \ln K_{RR} \quad (1a)$$

$$\Delta G_{RP} = -NkT \ln K_{RP} \quad (1b)$$

$$\Delta G_{PP} = -NkT \ln K_{PP} \quad (1c)$$

In a copolymer, RR, RP, and PP interactions occur with probabilities p_{RR}, p_{RP}, and p_{PP}, respectively. The resulting free

energy change for copolymer formation can be written as

$$\Delta G_{copol} = -NkT(p_{RR} \ln K_{RR} + p_{RP} \ln K_{RP} + p_{PP} \ln K_{PP}) \quad (2)$$

Let

$$K_{RP} = \alpha_{RP} K_{RR}$$

$$K_{PP} = \alpha_{PP} K_{RR}$$

Equation 2 can be written as

$$\Delta G_{copol} = -NkT\ [\ln K_{RR} + \ln (\alpha_{RP})^{p_{RP}} + \ln (\alpha_{PP})^{p_{PP}}] \quad (3)$$

The apparent equilibrium association constant for copolymer formation, K_{app}, is given by

$$K_{app} = K_{RR}(\alpha_{PR})^{p_{RP}}(\alpha_{PP})^{p_{PP}} \quad (4)$$

In a copolymer containing a proportion θ of P subunits, [respectively $(1 - \theta)$ of R subunits], the probabilities for R–R, R–P, and P–P interaction will be

$$p_{RR} = (1 - \theta)^2 \quad (5a)$$

$$p_{RP} = 2\theta(1 - \theta) \quad (5b)$$

$$p_{PP} = \theta^2 \quad (5c)$$

It is implicitly assumed, in eqs 2–5, that P–R and R–P interactions are energetically identical. This is an oversimplification, of course, since F-actin filaments are polar.[3] The average value of K_{RP} considered in eq 2 is the square root of the product of the intrinsic constants $K'_{RP}K'_{PR}$. Within this simplification, eq 4 can be written as

$$K_{app} = K_{RR}(\alpha_{PR})^{2\theta(1-\theta)}(\alpha_{PP})^{\theta^2} \quad (6)$$

K_{RR} and K_{app} are the reciprocals of the critical concentrations for polymers of unmodified actin and for copolymers containing a proportion θ of PLP–actin subunits, respectively. Equation 6 can also be written as

$$C_{c\,app} = C_{co}\left(\frac{1}{\alpha_{PR}}\right)^{2\theta(1-\theta)}\left(\frac{1}{\alpha_{PP}}\right)^{\theta^2} \quad (7)$$

Data showing the dependence of $C_{c\,app}$ on θ are summarized in Table I and have been further analyzed according to eq 7. The proportion of PLP–actin subunits in the copolymers, θ, was calculated assuming that the increase in the apparent critical concentration upon addition of increasing amounts of PLP–actin to a constant amount of regular actin was essentially due to PLP–actin. This assumption is justified both by examination of the results displayed in Figure 7, which show that essentially the same amount of unmodified actin polymerizes independently of the presence of PLP–actin, and by consideration of the laws of random copolymerization developed by Oosawa (1975), according to which in a copolymer of monomer species 1 and 2 the partial critical concentration of monomer 1 decreases upon an increase of the concentration of monomer 2 in the mixture. In the present case, the partial critical concentration of unmodified actin decreases from 0.15 μM to 0. Experimental data were satisfactorily accounted for by eq 7 using values of 0.02 and 0.005 for α_{RP} and α_{PP}, respectively, and a value of 0.15 μM for $C_{co} = 1/K_{RR}$. From

[3] It is also an oversimplification to consider that actin–actin interactions can be of three types as mentioned above, as if F-actin was a linear polymer, while in fact each subunit in the filament interacts with four neighbors, and the exact mathematical description of the system is much more complex.

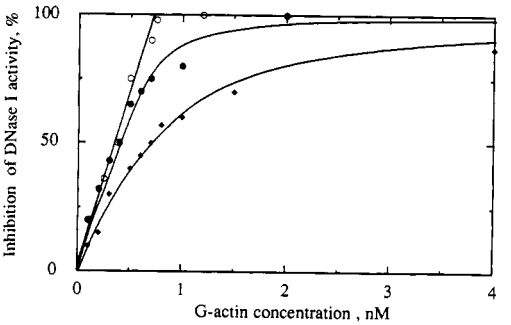

FIGURE 8: Interaction of PLP–G-actin and unmodified G-actin with DNase I. The G-actin concentration dependence of the catalytic activity of DNase I was measured first at a high DNase I concentration. The percent of inhibition of DNase I by G-actin varied strictly linearly with G-actin concentration up to 1 mol of G-actin/mol of DNase I. These data were then plotted (○) on a 40-fold lower G-actin concentration range, leading to the ideal stoichiometric titration line that would be obtained, at a 40-fold lower DNase I concentration, if the affinity of G-actin for DNase I was infinite. The percent of inhibition of DNase I activity by G-actin (●) or PLP–G-actin (◆) was effectively measured at this 40-fold lower DNase I concentration. The data yielded hyperbolic saturation curves consistent with the formation of a 1:1 complex DNase I–G-actin (●) or DNase I–PLP–G-actin (◆). Solid lines are the corresponding calculated binding isotherms using values of 0.05 nM and 0.4 nM for the equilibrium dissociation constants of the DNase I–G-actin and DNase I–PLP–G-actin complexes, respectively.

these numbers, the critical concentration for polymerization of pure PLP–actin is $K_{PP}^{-1} = (\alpha_{PP}K_{RR})^{-1} = 30$ μM, which is in agreement with the observations. The data also indicate that a copolymer in which only RP and PR contacts exist should polymerize with an apparent critical concentration equal to $(K'_{RP}K'_{PR})^{-1/2} = 0.15/0.02 = 7.5$ μM. Data in Figure 5 show that PLP–actin binds to the barbed end of unmodified F-actin filaments with an equilibrium dissociation constant of 4 μM; therefore, $K'_{PR} = 0.25$ μM^{-1}.

PLP-Actin Binds to DNase I with an Affinity 10-fold Lower Than That of Unmodified Actin. G-actin is well-known to bind DNase I tightly, with a reported equilibrium dissociation constant of 1–2 nM (Mannherz et al., 1980; Pinder & Gratzer, 1982). However, these values were often determined under conditions where the concentrations of actin and DNase I were 1–2 orders of magnitude higher than the derived equilibrium dissociation constant. To avoid these difficulties, the inhibition of DNase I activity by G-actin was measured under two different conditions: first in the presence of a known large amount of DNase I as compared to the equilibrium dissociation constant, and then in the presence of a 40-fold lower concentration. The first experiment yielded a linear actin concentration dependence of the percent of inhibition of DNase I activity up to 1 equivalent amount of actin, corresponding to the stoichiometric 1:1 titration of the actin–DNase I complex. From this experiment, the stoichiometric 1:1 titration curve of DNase I by G-actin at a 40-fold lower concentration of DNase I was derived, by dividing the actin concentration scale by 40 (open circles in Figure 8). The second experiment yielded a saturation curve that deviated from this stoichiometric line. From the two curves, the equilibrium dissociation constant K_D for the actin–DNase I complex could be derived. Note that knowledge of the actual concentrations of DNase I in the two assays is not necessary to derive the value of the equilibrium dissociation constant, only the ratio of these concentrations is needed. Data shown in Figure 8 can be described within hyperbolic binding isotherms for binding of unmodified actin and PLP–actin to DNase I, with equilibrium dissociation constants of 0.05 nM and 0.4 nM, respectively. The affinity of DNase I for actin therefore appears an order

of magnitude higher than previously determined. The modification of lysine-61 by PLP weakens the affinity of actin for DNase I by one order of magnitude; however, the complex remains appreciably tight. It is known that lysine-61 is part of the DNase I binding site (Sutoh, 1984; Kabsch et al., 1990). Previous modifications of this lysine affected the interaction of actin with DNase I to variable extents in the different reports (Burtnick, 1984; Ng & Burtnick, 1982; Miki, 1987). In view of the above results, these discrepancies might reflect the different ranges of concentrations of actin and DNase I in which binding measurements were made.

The interaction between PLP–actin and DNase I can also be monitored by PLP fluorescence. Pyridoxamine phosphate conjugates are known to fluoresce at 400 nm when excited in the 300–360-nm region (Churchich, 1965). Upon binding to DNase I, the fluorescence of PLP–actin (excitation 355 nm, emission 400 nm) was quenched by 11%. This property was used to titrate the PLP–actin–DNase I complex in the micromolar range. Data (not shown) were also consistent with the formation of a tight 1:1 complex between DNase I and PLP–actin with an equilibrium dissociation constant lower than 1 μM.

Polymerization of PLP–Actin Induced by Myosin Subfragment 1 (S_1A_1 Isomer). It is known that the isomer S_1A_1 of myosin subfragment 1 coassembles with G-actin, even in low ionic strength buffers, into F-actin–S_1 arrowhead-decorated filaments (Miller et al., 1988b), in which the actin–S_1 stoichiometry is 1:1 (Sutoh, 1983; Chen et al., 1985). The critical concentration for polymerization of F-actin–S_1 is too small to have been measured and is certainly lower than 0.05 μM. Similar very stable F-actin–S_1 filaments also assemble upon interaction of G-actin with the S_1A_2 isomer of S_1, except at a slower rate (Valentin-Ranc et al., 1991). In order to understand the mechanism of F-actin–S_1 filament assembly in detail, it is interesting to compare the S_1-induced polymerization of unmodified and PLP-modified actin. Light scattering was used to monitor the formation of decorated filaments. Figure 9A shows that in low ionic strength buffer (buffer G) PLP–G-actin did not form F-actin–S_1 decorated filaments, while control samples of unmodified G-actin displayed a large increase in light scattering upon addition of S_1A_1, consistent with the formation of F-actin–S_1 filaments. In the presence of 0.1 M KCl, however, PLP–G-actin polymerized upon addition of S_1A_1 (Figure 9B). The critical concentration for PLP–F-actin–S_1 decorated filaments was found to be 4.5 μM in repeated experiments at 20 °C and pH 7.8, a very high value as compared to the undetectable critical concentration for assembly of standard F-actin–S_1 filaments. F-Actin–S_1 and PLP–F-actin–S_1 filaments were sedimented. Gel electrophoresis of the material in the pellets, shown in Figure 9C, demonstrated that the actin:S_1 stoichiometry in the polymers was 1:1 in both cases.

The detailed mechanism of the polymerization of G-actin into decorated filaments induced by S_1 is still controversial, and the nature of the kinetic intermediates in the polymerization pathway is unknown. It was first proposed that the polymerization was not nucleated (Miller et al., 1988b), while another study favored a nucleated mechanism (Chaussepied & Kasprzak, 1989). We showed that tight ternary G_2S and binary GS complexes were the first species formed between G-actin and S_1 before the onset of polymerization. We also showed that the G_2S complex was formed between PLP–G-actin and S_1, with unaltered affinity (Valentin-Ranc et al. 1991). Notwithstanding the ignorance of the detailed sequence of elementary reactions leading to the final F-actin–S_1 complex, we can propose a hypothetic simple scheme accounting for the results: in this model, PLP–G-actin (P) interacts with S_1 (S) to form a PS complex with an equilibrium dissociation K. The PS complex polymerizes then into $(PS)_n$, with a po-

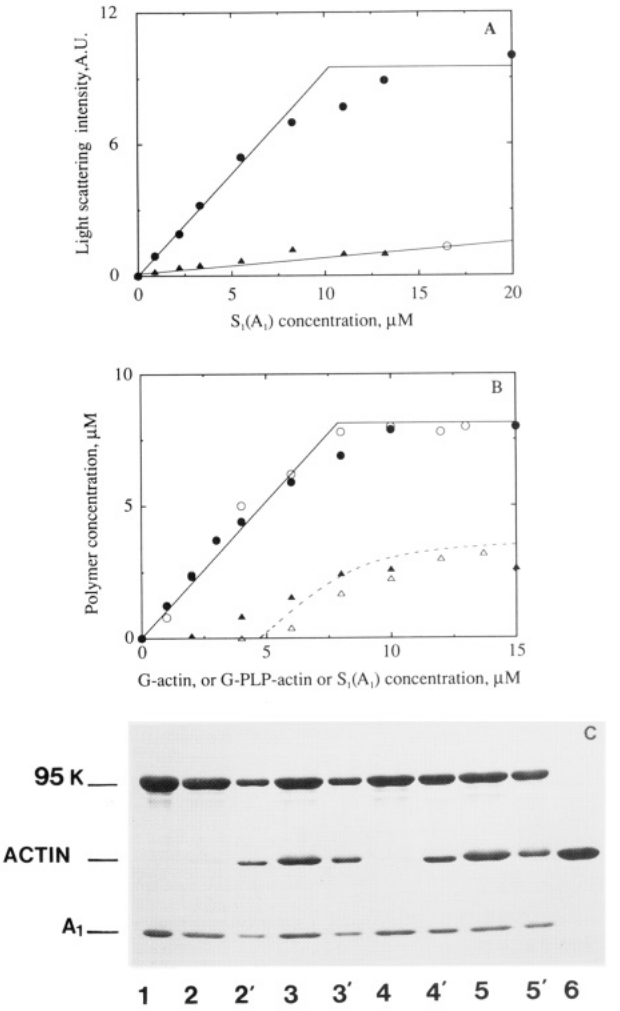

FIGURE 9: Interaction of PLP–G-actin with myosin subfragment 1 (S_1A_1). The time course of polymerization of F-actin–S_1 decorated filaments was monitored by light scattering at 600 nm (see Materials and Methods). In panels B and C, the concentration of polymer formed (in millimolar concentrations of either actin or S_1 in the F-actin–S_1 polymer) has been derived from the increase in light scattering measured at the end of the polymerization reaction. Panel A: Polymerization of F-actin–S_1 in G buffer. S_1A_1 at the indicated concentrations was added to G-actin (●) or PLP–G-actin (▲) at 8 μM. At all S_1 concentrations, G-actin was polymerized in less than 5 min, and closed circles represent light-scattering measurements made when the plateau was reached. No polymerization was observed with PLP–G-actin for up to 50 min; therefore, triangles represent light-scattering measurements made at time 50. The open circle represents the light-scattering intensity measured for S_1A_1 alone at 16 μM. Panel B: Polymerization of F-actin–S_1 in F buffer. This is the same experiment as in panel A, except it was done in polymerization buffer (F buffer is G buffer supplemented with 0.1 M KCl). Closed symbols represent S_1A_1 at the indicated concentrations added to either G-actin (●) or PLP–G-actin (▲) at 8 μM. Open symbols represent G-actin (○) or PLP–G-actin (△) added at the indicated concentrations to 8 μM S_1A_1. The dashed line is the theoretical curve calculated according to eq 10, using $K = 0.4$ μM and $K_p = 4.5$ μM. Panel C: Electrophoretic patterns of F-actin–S_1 filaments sedimented in the ultracentrifuge. Samples from the experiment described in panel B were centrifuged for 10 min at 350000g in the Beckman TL100 ultracentrifuge. Supernatants (lanes i) and pellets (*lanes i′*) were electrophoresed on SDS–polyacrylamide gels (see Materials and Methods). All samples contained 8 μM S_1A_1 and the following amounts of actin: 2 and 2′, 2 μM G-actin; 3 and 3′, 10 μM PLP–G-actin; 4 and 4′, 3 μM G-actin; 5 and 5′, 12 μM PLP–G-actin. Lanes 1 and 6 represent S_1A_1 and G-actin alone, respectively.

lymerization constant K_p. This model is described by the following equations:

$$P + S \rightleftarrows PS \qquad (K) \tag{8a}$$

$$(PS)_n + PS \rightleftarrows (PS)_{n+1} \qquad (K_p) \tag{8b}$$

If P_o and S_o represent the total concentrations of PLP–actin and S_1, respectively, then at equilibrium

$$[PS]_{eq} = K_p \tag{9a}$$

$$[P]_o = [P] + K_p + c_w \tag{9b}$$

$$[S]_o = [S] + K_p + c_w \tag{9c}$$

where c_w is the concentration of polymerized PS expressed in molar amount of either P or S. The dependence of c_w on the total concentrations of PLP actin $[P]_o$ and S_1A_1 $[S]_o$ is described, within this model, by the following equation:

$$c_w = ([P]_o + [S]_o - 2K_p - \sqrt{([P]_o - [S]_o)^2 + 4KK_p})/2 \tag{10}$$

The data in Figure 9B can be described satisfactorily by eq 10. The best fit was obtained using values of 4.5 μM and 0.4 μM for K_p and K, respectively. These numbers indicate that PLP modification of actin causes a much larger alteration in actin–actin interactions than in actin–S_1 interactions in agreement with other observations (Valentin-Ranc et al., 1991).

Discussion

The results reported in this paper show that the lysine-specific reagent pyridoxal 5′-phosphate reacts with 1.7–2.0 lysines on average on G-actin. Limited proteolytic digestion by thrombin and α-chymotrypsin indicates that, in agreement with previous works, lysine-61 is the most reactive of the lysines on G-actin, and is modified in a 1:1 ratio by PLP. The remainder of covalently incorporated PLP appears scattered on different lysines that are each labeled with a low stoichiometry. Therefore, although a low-level modification of other lysines could not be avoided, the fact that lysine-61 is modified on all G-actin molecules leads to the conclusion that PLP–G-actin can be considered as a homogeneous well-defined actin variant, whose properties are linked to the covalent modification of lysine-61. This view is supported by the data, which show that PLP–actin has a greatly reduced ability to polymerize into filaments, its critical concentration being increased approximately 200-fold, which corresponds to a 2.8 kcal/mol energetic difference in actin–actin interactions. PLP–actin keeps the same ATP binding properties and sedimentation coefficient as unmodified actin. Lysine-61 is known to be exposed at the pointed end of the actin molecule, on top of subdomain 2 (Kabsch et al., 1990), which interacts with subdomain 1 of the adjacent subunit along the long pitch helix of the filament, and also is part of the interaction area with DNase I (Holmes et al., 1990; Podolski & Steck, 1988). Interestingly, modifying lysine-61 on G-actin causes a 10-fold decrease in its affinity for DNase I or for the barbed ends of filaments but does not affect the rate of ATP exchange or the reactivity of Cys-374, since PLP–actin can be pyrenyl-derivatized like unmodified actin. Other data (Valentin-Ranc et al., 1991) also indicate that the interaction of G-actin with myosin subfragment 1 is not affected by PLP modification. Therefore, labeling of lysine-61 specifically affects the region of the actin molecule that is involved in longitudinal actin–actin interactions along the long pitch helix of the filament. Although unable to self-assemble, PLP–actin can copolymerize with unmodified actin. A simple correlation could be established between the apparent critical concentration for copolymer formation and the fraction of PLP–actin subunits in the filament. The fact that the data can be quantitatively accounted for by a simple model strengthens the view that PLP-modified actin behaves like a homogeneous species. The results point out the potential interest in obtaining a filament in which longitudinal actin–actin interactions are specifically and quantitatively modified in a controlled fashion, by varying the fraction of PLP subunits in the polymer. PLP–actin will therefore provide a useful tool for approaching the role of actin structure and dynamics in the movement of myosin along actin filaments.

Upon interaction with myosin subfragment 1 (S_1A_1 isomer), PLP–actin assembles into F-actin–S_1 decorated filaments, in the presence of 0.1 M KCl. These filaments have the same 1:1 actin:S_1 stoichiometry as those formed from unmodified actin; however, the critical concentration for assembly is much higher (4.5 μM) than that of regular F-actin–S_1. Regarding S_1-induced polymerization of actin, the difference between unmodified actin and PLP–actin is even larger in low ionic strength buffers in which no polymerization of F-actin–PLP–S_1 filaments has been observed at concentrations up to 10 μM for each protein. The polymerization data are quantitatively consistent with the view that (1) PLP modification does not affect the binding of S_1 to G-actin, in agreement with our recent report (Valentin-Ranc et al., 1991) and (2) the binding of S_1 to actin strengthens the actin–actin interactions in the filament, i.e., decreases the critical concentration for polymerization. PLP–actin therefore will be useful in analyzing the mechanism of actin–S_1 polymerization and in characterizing the intermediate complexes involved in the polymerization process.

Acknowledgments

We thank Dr. D. Pantaloni for help in image analysis of the gels of digested actin (Figures 2 and 3) and for stimulating discussions throughout the work.

Registry No. DNase I, 9003-98-9; Lys, 56-87-1; ATP, 56-65-5.

References

Bettache, N., Bertrand, R., & Kassab, R. (1989) *Proc. Natl. Acad. Sci. U.S.A. 86*, 6028–6032.

Blikstad, I., Markey, F., Carlsson, L., Persson, T., & Lindberg, U. (1978) *Cell 15*, 935–943.

Burtnick, L. D. (1984) *Biochim. Biophys. Acta 791*, 57–62.

Carlier, M.-F., Pantaloni, D., & Korn, E. D. (1984) *J. Biol. Chem. 259*, 9983–9986.

Carlier, M.-F., Pantaloni, D., & Korn, E. D. (1985) *J. Biol. Chem. 260*, 6565–6571.

Carlier, M.-F., Criquet, P., Pantaloni, D., & Korn, E. D. (1986) *J. Biol. Chem. 261*, 2041–2050.

Chaussepied, P., & Kasprzak, A. A. (1990) *Nature 342*, 950–953.

Chen, T., Applegate, D., & Reisler, E. (1985) *Biochemistry 24*, 137–144.

Churchich, J. E. (1965) *Biochim. Biophys. Acta 102*, 280–288.

Dempsey, W. B., & Snell, E. E. (1963) *Biochemistry 2*, 1414–1420.

Eisenberg, E., & Kielley, W. W. (1974) *J. Biol. Chem. 249*, 4742–4748.

Frieden, C., & Patane, K. (1988) *Biochemistry 27*, 3812–3820.

Fry, D. C., Kuby, S. A., & Mildvan, A. S. (1986) *Proc. Natl. Acad. Sci. U.S.A. 83*, 907–911.

Gordon, D. J., Yang, Y.-Z., & Korn, E. D. (1976) *J. Biol. Chem. 251*, 7474–7479.

Greene, L. E. (1984) *J. Biol. Chem. 259*, 7363–7366.
Heaphy, S., & Tregear, R. (1984) *Biochemistry 23*, 2211–2214.
Hill, T. L. (1987) in *Linear Aggregation Theory in Cell Biology*, pp 110–121, Springer-Verlag, New York.
Hitchcock, S. E., Carlsson, L., & Lindberg, U. (1976) *Cell 7*, 531–542.
Hitchcock-De Gregori, S., Mandala, S., & Sachs, G. A. (1982) *J. Biol. Chem. 257*, 12573–12580.
Holmes, K. C., & Kabsch, W. (1991) *Curr. Opin. Struct. Biol. 1*, 270–280.
Holmes, K. C., Popp, D., Gebhard, W., & Kabsch, W. (1990) *Nature 347*, 44–49.
Kabsch, W., Mannherz, H. G., Suck, D., Pai, E. F., & Holmes, K. C. (1990) *Nature 347*, 37–44.
Konno, K. (1987) *Biochemistry 26*, 3582–3589.
Konno, K. (1988) *J. Biochem. 103*, 386–392.
Kouyama, T., & Mihashi, K. (1981) *Eur. J. Biochem. 114*, 33–38.
Kunitz, M. (1950) *J. Gen. Physiol. 33*, 363–377.
Laemmli, U. K. (1970) *Nature 227*, 680–685.
Lu, R. C., & Szilagyi, L. (1981) *Biochemistry 20*, 5914–5919.
Mannherz, H. G., Goody, R. S., Konrad, M., & Nowak, E. (1980) *Eur. J. Biochem. 104*, 367–379.
Margossian, S. S., & Lowey, S. (1982) *Methods Enzymol. 85B*, 55–71.
Matsuo, Y. (1957) *J. Am. Chem. Soc. 79*, 2011–2020.
McLean Fletcher, S., & Pollard, T. D. (1980) *Biochem. Biophys. Res. Commun. 96*, 18–27.
Miki, M. (1987) *Eur. J. Biochem. 164*, 229–235.
Miki, M. (1989) *J. Biochem. (Tokyo) 106*, 651–655.
Miki, M., & Dos Remedios, C. G. (1988) *J. Biochem. (Tokyo) 104*, 232–235.
Miller, L., Phillips, M., & Reisler, E. (1988a) *Eur. J. Biochem. 174*, 23–29.
Miller, L., Phillips, M., & Reisler, E. (1988b) *J. Biol. Chem. 263*, 1996–2002.
Mornet, D., & Ue, K. (1984) *Proc. Natl. Acad. Sci. U.S.A. 81*, 3680–3684.
Muszbek, L., Gladner, J. A., & Laki, K. (1975) *Arch. Biochem. Biophys. 167*, 99–103.
Ng, J. S. Y., & Burtnick, L. D. (1982) *Int. J. Biol. Macromol. 4*, 215–218.
Nowak, E., & Goody, R. (1988) *Biochemistry 27*, 8613–8617.
Offer, G., Moos, C., & Starr, R. (1973) *J. Mol. Biol. 74*, 653–676.
Oosawa, F. (1975) in *Thermodynamics of the Polymerization of Protein*, Academic Press, London.
Pinder, J. C., & Gratzer, W. B. (1982) *Biochemistry 21*, 4886–4890.
Podolski, J. L., & Steck, T. L. (1988) *J. Biol. Chem. 263*, 638–645.
Spudich, J. A., & Watt, S. (1971) *J. Biol. Chem. 246*, 4866–4871.
Sutoh, K. (1983) *Biochemistry 22*, 1579–1585.
Sutoh, K. (1984) *Biochemistry 23*, 1942–1946.
Tamura, J. K., Rakov, R. D., & Cross, R. L. (1986) *J. Biol. Chem. 261*, 4126–4133.
Toyoshima, Y. Y., Kron, S. J., Mc Nally, E. M., Niebling, K. R., Toyoshima, C., & Spudich, J. A. (1987) *Nature 328*, 536–539.
Valentin-Ranc, C., Combeau, C., Pantaloni, D., & Carlier, M.-F. (1991) *J. Biol. Chem. 266*, 17872–17879.
Waring, A. J., & Cooke, R. (1987) *Arch. Biochem. Biophys. 252*, 197–205.
Weeds, A. G., & Taylor, R. S. (1975) *Nature 257*, 54–56.
Weeds, A. G., & Pope, B. (1977) *J. Mol. Biol. 111*, 129–157.